3D NMR Characterization of Chain Ends Formed by Phosphinyl Radical Initiated Polymerization of Styrene

Huihan Meng, Takeshi Saito, and Peter L. Rinaldi*,†

Knight Chemical Laboratory, Department of Chemistry, The University of Akron, Akron, Ohio 44325-3601

Faith Wyzgoski, Carin A. Helfer, Wayne L. Mattice,* and H. James Harwood*

Maurice Morton Institute of Polymer Science, The University of Akron, Akron Ohio 44325-3909

Received May 23, 2000; Revised Manuscript Received November 13, 2000

ABSTRACT: Pulsed field gradient, triple resonance, and three-dimensional (3D) NMR techniques at 750 MHz were used to study the initiation mechanism and to characterize the polymer chain end structures obtained by radical initiation of styrene polymerization with (2,4,6-trimethylbenzoyl)diphenylphosphine oxide (TPO). Additional polystyrene samples were prepared from α-d_1-styrene and β,β-d_2-styrene, and these samples were studied by 3D SQ-HCAP experiments. The results suggest that all the chain-end structures are formed by the addition of phosphinyl radical to the methylene carbon of styrene. 3D-NMR permitted resolution of resonances of chain-end structures up to the tetrad level. With the help of molecular simulation and RIS calculations, the resonances of C_α on the chain-end structures were assigned up to the triad level. Poly(α,β-$^{13}C_2$-styrene) was prepared by TPO initiation, and its chain-end structures were characterized by the combined use of 3D SQ-HCAP and CT-HCCH experiments.

Introduction

Nuclear magnetic resonance has been proven to be a valuable tool for analyzing polymer chain-end groups. In the past, ^{13}C NMR was mostly used for analysis of polymer chain-end groups. For example, Moad et al.[1] used ^{13}C NMR to identify incorporated initiator fragments, and Bevington et al.[2,3] reported studies of the nature and stereochemistry of monomeric units near the chain ends of the polymers. The big limitation of this method is the low concentration of chain-end groups relative to backbone groups. Commonly, ^{13}C-enriched initiators[4] are used to overcome this problem. This enhances the signals generated from chain-end initiator fragments relative to the signals from the rest of the polymer backbone.

However, there is still a problem involving overlap of the chain end and backbone resonances. To solve this problem, initiator and chain transfer agents containing high natural abundance nuclei such as ^{31}P or ^{19}F could be used to generate the chain ends.[5,6] One can observe these nuclei instead of ^{13}C by using heteronuclear one-dimensional (1D) and multidimensional NMR.

It is well-known that polymerization employing radiation technology has many advantages such as speed, efficiency and utilization of solvent-free systems. Among the radical initiators used, (2,4,6-trimethylbenzoyl)-diphenyphosphine oxide (TPO) has the ability to absorb light in the near UV, is efficient, and is stable toward hydrolysis.[7] Studies of monoacylphosphine oxides by Schnabel and co-workers[8] have shown that these types of initiators undergo α-cleavage from the triplet state to produce an aroyl−phosphinyl radical pair. Each radical of the pair is capable of initiating polymerization. However, the diphenylphosphinyl radical ($Ph_2P(O)^\bullet$) is 1−2 orders of magnitude more reactive than the benzoyl radical toward vinyl monomers. Radical trapping techniques[9] and 1-D NMR studies[5] have yielded additional data on the high reactivity of the diphenylphosphinyl radical. Since most of the initiated chain ends of the polystyrene contain ^{31}P nuclei, this enables one to characterize the chain end by ^{31}P NMR and ^{31}P-related 3D NMR experiments.

The ^{31}P resonances from these polymers are quite broad and subtle structural information is hidden within these broad signals. 1D ^{31}P NMR still has limitations when attempting to resolve signals from chain-end structures and to obtain information about the tacticity and stereochemistry of the chain-end groups. To solve this problem, Rinaldi and Saito[10] used ^{1}H/^{13}C/^{31}P triple resonance pulsed field gradient (PFG) NMR methods, which can be enormously useful for chain-end structure characterization. In this paper, research work based on chain-end characterization of polystyrenes formed by initiation with TPO are reported. A series of ^{1}H/^{13}C/^{31}P triple resonance 3D NMR spectra were collected. Polystyrenes substituted with deuterium on either their methylene or methine carbons were used to aid in the identification of the carbon (C_α) bonded to ^{31}P at their chain ends. Additionally, ^{13}C-labeled polystyrene formed by initiation with TPO was investigated. 3D NMR spectra of this polymer permitted identification of the backbone styrene carbon (C_β and C_γ) resonances of the first two monomer units of the ^{31}P-containing chain end.

Experimental Section

General Synthesis. Polymerization of Styrene. (2,4,6-Trimethylbenzoyl)diphenylphosphine oxide (Lucirin TPO) was kindly provided by BASF. Styrene (Aldrich) was distilled prior to use; α-d_1-styrene, β,β-d_2-styrene and α,β-$^{13}C_2$-styrene were obtained from Isotec, Inc., and were purified by elution through HQ/MEHQ inhibitor-removing sieves (Aldrich). TPO-initiated

† Telephone: 330-972-5990. Fax: 330-972-5256. E-mail: PeterRinaldi@uakron.edu.

10.1021/ma000898c CCC: $20.00
Published on Web 01/16/2001

radical polymerization of styrenes was conducted by irradiation with 500 W tungsten light source. A glass vial containing a magnetic stir bar, monomer, anhydrous benzene (Aldrich), and TPO was closed with a crimp-seal cap equipped with a Teflon-coated butyl rubber septum, purged with argon and irradiated for 3 h. The temperature of the reaction mixture did not exceed 35 °C. After concentration, the mixture was precipitated into hexanes. Polymers thus obtained were purified by reprecipitation from tetrahydrofuran (THF)−hexanes. A 121 MHz ^{31}P NMR spectrum of the polymer in chloroform-*d* was obtained to verify that unreacted TPO (singlet, $\delta = 13.8$; lit.[11] $\delta = 14.18$) was removed. The molecular weights of the polymers were measured by GPC (a Waters 510 pump, equipped with Waters Styragel columns HR1, HR4E, and HR5E (each 7.8 × 300 mm) employed in sequence, Waters 410 differential refractometer, using THF as eluent) calibrated by polystyrene standards.

Polystyrene was prepared using TPO (0.4561 g, 1.5 mol % based on monomer), anhydrous benzene (10.0 mL), and styrene (9.09 g, 0.087 mol). Three reprecipitations from THF−hexanes were conducted. The M_n of the polymer was 9030, and its polydispersity (M_w/M_n) was 1.8. Yield: 1.22 g (13.4%). Poly(α-d_1-styrene)[12] was prepared using TPO (0.06922 g, 0.76 mol % based on monomer), benzene (3 mL), and α-d_1-styrene (2.76 g, 0.0262 mol). Two reprecipitations were conducted. The M_n of the polymer was 8260, and its polydispersity was 1.71. Yield: 0.248 g (9.0%). Poly(β,β-d_2-styrene) was prepared using TPO (0.0684 g, 0.76 mol % based on monomer), anhydrous benzene (3 mL), and β,β-d_2-styrene (2.76 g, 0.026 mol). Two reprecipitations were conducted. The M_n of the polymer was 10 300, and its polydispersity was 1.67. Yield: 0.262 g (9.5%). Poly(α,β-$^{13}C_2$-styrene) was prepared using TPO (0.0246 g, 0.79 mol % based on monomer), anhydrous benzene (3 mL) and α,β-$^{13}C_2$-styrene (0.9534 g, 0.00898 mol). One reprecipitation was conducted. The M_n of the polymer was 5480, and its polydispersity was 1.66. Yield: 0.0974 g (10.2%).

General NMR. All the NMR spectra were obtained with a Varian UnityPlus-750 MHz spectrometer equipped with Ultrashims, a pulsed field gradient accessory, and a Varian 5 mm ^{1}H/^{13}C/^{31}P PFG triple resonance probe, unless cited otherwise. The temperature was regulated at 25 ± 0.1 °C. All the data processing was performed on a Sun SPARCstation-10 using Varian's Vnmr software.

Spectra of polystyrene, poly(α-d_1-styrene), poly(β, β-d_2-styrene), and poly(α,β-$^{13}C_2$-styrene) were obtained from 100 mg samples dissolved in 0.7 mL of $CDCl_3$ contained in 5 mm NMR tubes.

1D NMR Experiments. The ^{1}H spectra were obtained with the following parameters: a 2.8 μs (∼30°) ^{1}H pulse width, an 8000 Hz spectral window, a 1.8 s acquisition time, four transients and no relaxation delay. The ^{13}C spectra were collected with a Varian 5 mm broad band (BB) probe, which can be tuned to frequencies between the resonances of ^{31}P and ^{15}N. The following parameters were used: a 40774.0 Hz spectral window, a 5.2 μs (∼45°) ^{13}C pulse width, a 1.0 s acquisition time, a 4.0 s relaxation delay, 8192 transients, and WALTZ-16 ^{1}H decoupling with a field strength of 2.8 kHz during the acquisition time. The ^{31}P spectra were collected on a Varian VXR 300 MHz spectrometer with the parameters as follows: a 8984 Hz spectral window, an 8.7 μs (∼45°) pulse width, a 1.0 s relaxation delay, 10240 transients, and a 1.0 s acquisition time, with ^{1}H WALTZ-16 decoupling throughout the experiments using a field strength of 2.2 kHz. The chemical shifts were externally referenced to standard concentrated phosphoric acid solution (0 ppm).

3D SQ-HCAP Experiments.[10] The HCAP pulse sequence is analogous to the HNCA sequence [13] used in biological NMR. Here, the 3D correlation relates the shift of the α-^{13}C nucleus with those of the directly bonded ^{1}H and ^{31}P atoms. The spectra were obtained using the following parameters: ^{1}H, ^{13}C, and ^{31}P 90° pulse widths of 9.0, 14, and 56 μs, respectively; 2246.6, 1320.3, and 1517.8 Hz spectral windows in the ^{1}H (f_3), ^{13}C (f_2), and ^{31}P (f_1) dimensions; a 1.0 s relaxation delay; and a 0.048 s acquisition time with ^{13}C GARP-1[14] decoupling using a field strength of 5.5 kHz. Eight transients were averaged for each of the 36 complex t_1 (^{31}P) and 48 complex t_2 (^{13}C) increments; The delays were set to $\Delta = (4 \times {}^1J_{HC})^{-1} = 1.78$ ms, $\tau = (4 \times {}^1J_{CP})^{-1} = 4.17$ ms, respectively. Gradients g_1 and g_2 were each applied for 1.0 and 1.0 ms with strengths of 0.562 and 0.140 T m^{-1}, respectively. These PFGs provide coherence selection between ^{13}C and ^{1}H nuclei. The total acquisition time was about 18 h. Linear prediction was used to forward-extend the data in the t_1, t_2, and t_3 dimensions to twice the original size in each dimension (16 complex points were used to calculate four coefficients).

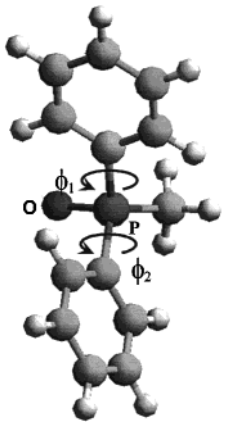

Figure 1. Optimized structure of the diphenylphosphinyl unit. ϕ_1 is defined, starting at the top ring, by the atoms $C_{ar}-C_{ar}-P-C_{CH3}$. ϕ_2 is defined, starting at the bottom ring, by $C_{ar}-C_{ar}-P-C_{CH3}$.

3D CT-HCCH Experiment.[15] The 3D CT-HCCH spectrum was obtained using the following parameters: 90° ^{1}H and ^{13}C pulse widths of 8.9 and 16 μs, respectively; 4149.8, 8298.8, and 5980.0 Hz spectral windows in the ^{13}C SQ (f_1), ^{13}C DQ (double quantum) (f_2) and ^{1}H (f_3) dimensions, respectively; a 1.0 s relaxation time; a 0.054 s acquisition time with ^{13}C MPF7[16] decoupling using a field strength of 4.28 kHz. Four transients were averaged for each of 60 complex t_1 and 64 complex t_2 increments; Decoupling on the ^{31}P channel was applied throughout the experiment using the MPF7 decoupling sequence with a field strength of 1.58 kHz. The PFGs g_1, g_2 and g_3 were applied for 3.0, 1.0, and 1.0 ms with strengths of 0.56, 0.45, and −0.22 T m^{-1}, respectively. The first PFG is a homospoil gradient used for purging undesired signals; the second and the third PFGs provide coherence selection between ^{13}C DQ and ^{1}H frequencies. The delays were optimized for $(4 \times {}^1J_{HC})^{-1} = 1.78$ ms, and the constant evolution time, CT was set to $(4 \times {}^1J_{CC})^{-1} = 7.14$ ms. The total experiment time was approximately 18 h. Digital signal processing (DSP) was applied to reduce the spectral window in the f_3 dimension from 5980 to 2990 Hz.

RIS Calculation and Molecular Simulation. The RIS model of Rapold and Suter,[17,18] with gauche states and *d*,*l* pseudoasymmetric centers[19] as defined by Mattice and Suter, was used to investigate the possible conformations of polystyrene triads. First, the optimized structure of the diphenylphosphinyl unit (Figure 1) was determined. The torsion angles for rotation of the phenyl rings, denoted ϕ_1 and ϕ_2, were varied from 0 to 180° at increments of 30°. Because of symmetry, the torsion angles from 180 to 360° did not need to be evaluated. In the optimized structure, the angles ϕ_1 and ϕ_2 are +123.5 and −11.7°, respectively. This unit was added to each of the preferred conformations of the polystyrene. The resulting structures were then optimized by using energy minimization calculations. The software program Cerius^2 (Version 3.5) from Molecular Simulations Inc., was employed to do all of the energy minimization calculations, which were done by using the Universal Force Field. The convergence criteria selected was a RMS displacement of 3.0×10^{-3} Å or an energy difference of 1.0×10^{-3} kcal/mol.

The evaluation of the degree of nonequivalence of the protons H_a and H_b on the methylene carbon directly bound

Scheme 1. Possible Chain-End Forming Reactions for TPO-Initiated Polystyrene

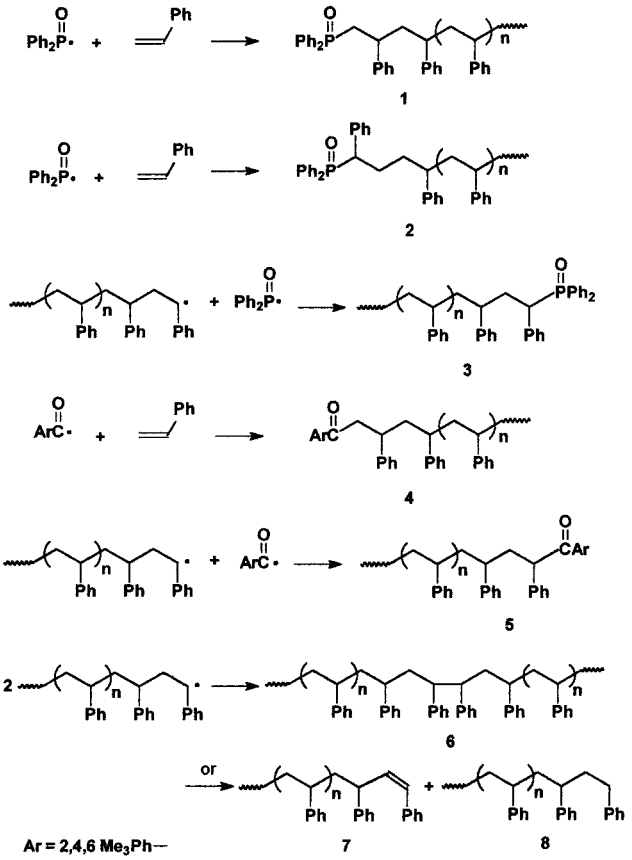

to the phosphorus atom, was performed by determining the ring currents for each proton as described by Bovey.[20] For each proton five separate ring current values, one arising from each of the five neighboring phenyl rings, were determined. These five ring currents were totaled, making the assumption that each proton feels an overall ring current effect from all of the phenyl rings. Therefore, for a given proton of a specific structure, a single ring current shielding value was obtained.

Results and Discussion

Polystyrene Structures from TPO Initiator. When diphenylphosphinyl radicals react with styrene monomers, the reactions can occur in several ways. The probable chain end structures are illustrated in Scheme 1. Structure **1** is expected to be the most dominant. It results from an initiation step that involves the addition of a diphenylphosphinyl radical to the unsubstituted end (β-carbon) of styrene. Structure **2** results from the initiation step involving addition of a diphenylphosphinyl radical to the substituted end (α-carbon) of styrene. Structure **3** comes from termination of a propagating polystyrene radical by coupling with a diphenylphosphinyl radical. In addition to these structures, polymer chain ends containing trimethylbenzoyl groups (**4** and **5**) are also expected. Additional termination reactions could involve coupling of two propagating polymer chain ends to form **6** or disproportionation to form **7** and **8**. The focus of this work was to study the role of phosphinyl radicals using NMR methods to probe the chain ends derived from them. Consequently, resonances from the trimethylbenzoyl-containing structure fragments and fragments from coupling or disproportionation were not studied in this work and are not discussed further.

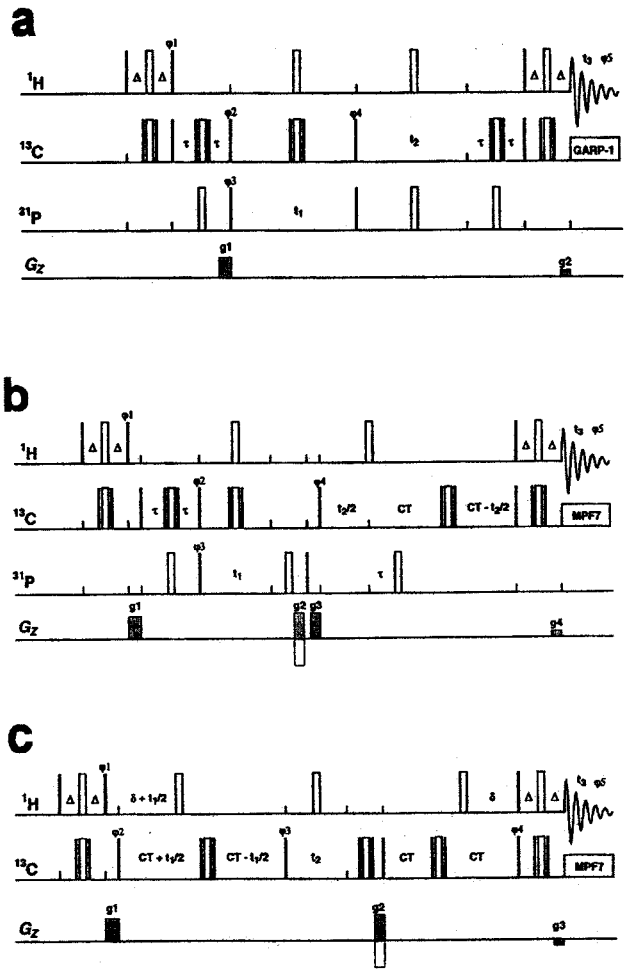

Figure 2. Pulse sequences for (a) SQ-HCAP, (b) CT-SQ-HCAP, and (c) CT-HCCH experiments.

NMR Pulse Sequences. The triple resonance 3D SQ-HCAP pulse sequence is shown in Figure 2a. The sequence involves sequential INEPT[21] magnetization transfer steps from ^{1}H to $^{13}C_\alpha$, from $^{13}C_\alpha$ to ^{31}P, ^{31}P chemical shift evolution during t_1, reverse INEPT transfer from ^{31}P to $^{13}C_\alpha$, ^{13}C chemical shift evolution during t_2, and finally reverse INEPT transfer from $^{13}C_\alpha$ to ^{1}H for detection of ^{1}H signals during t_3. These consecutive INEPT-type transfers act like a filter for selective detection of the ^{31}P-containing chain end groups while removing the rest of the signals. In other words, the f_2f_3 planes (^{1}H vs ^{13}C chemical shift) are more like HMQC[22] spectra, with the exception that the resonances of the CH_n groups not bound to ^{31}P have been filtered from the spectrum. When ^{13}C labeling is used, a constant time (CT = $^1/_2J_{CC}$) must be added during the ^{13}C chemical shift evolution time, see Figure 2b. In this way, we can remove ^{13}C−^{13}C homonuclear J coupling in this dimension and hence simplify the spectra.

Figure 2c shows a diagram of the CT-HCCH 3D experiment. In this experiment, an INEPT transfer from ^{1}H to ^{13}C replaces the first 90° ^{13}C pulse in the INADEQUATE 2D-NMR experiment.23 Then a reverse INEPT polarization transfer from ^{13}C back to ^{1}H is added at the end of the INADEQUATE sequence. The SQ-^{13}C chemical shift evolution occurs during t_1, DQ-^{13}C chemical shift evolves during t_2 and ^{1}H chemical shift evolution occurs during t_3. This DQ filtered HCCH

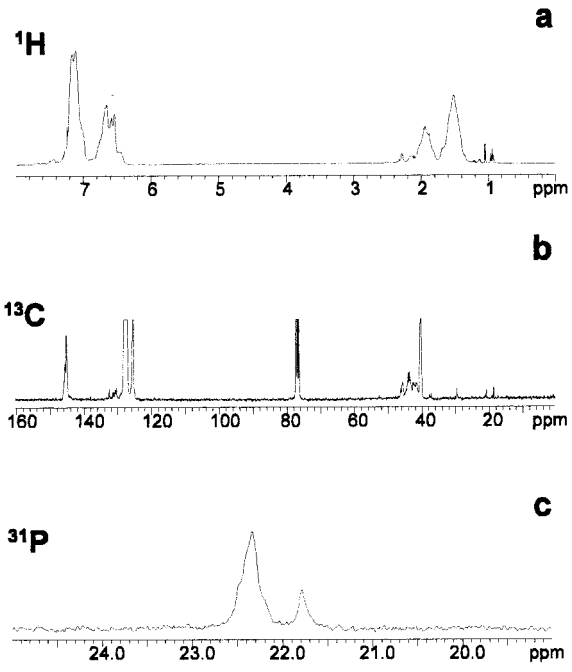

Figure 3. 1D NMR spectra of TPO-initiated polystyrene: (a) 750 MHz ^{1}H, (b) 188 MHz ^{13}C, and (c) 121 MHz ^{31}P.

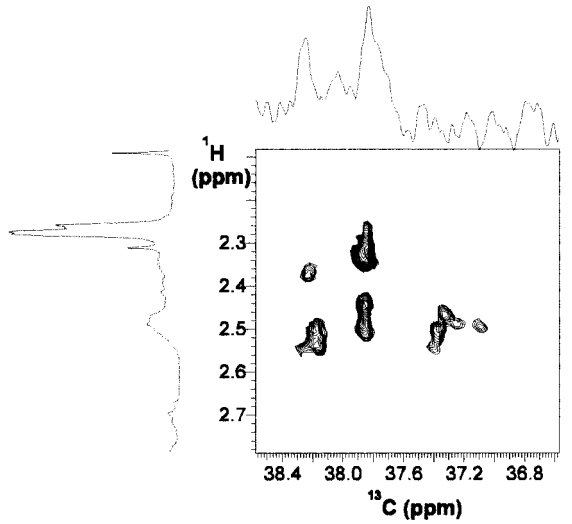

Figure 4. f_2f_3 (^{1}H−^{13}C) projection from the SQ-HCAP spectrum of TPO-initiated polystyrene.

experiment provides information much like the 2D INADEQUATE experiment. If a slice at one proton shift (f_3 dimension) is selected, this slice will contain the ^{13}C−^{13}C INADEQUATE correlations of the carbon bound to that proton.

The 1D ^{1}H, ^{13}C, and ^{31}P spectra of TPO-initiated polystyrene are shown in Figure 3. The chain-end ^{1}H and ^{13}C signals are just above the noise level and are much weaker than the main chain signals. Little information can be obtained from these spectra. The ^{31}P signals are strong but quite broad, hiding much of the structural information. Figure 4 shows the f_2f_3 (^{1}H−^{13}C) projection from SQ-HCAP spectra of TPO-initiated polystyrene. This 3D experiment disperses the ^{1}H and ^{13}C resonances into a third dimension based on the chemical shifts of the ^{31}P atoms to which they are attached. The projection of this spectrum onto the f_2f_3 plane will contain C−H correlations for these CHn groups bound to ^{31}P. Some of the ^{13}C signals (δ_C = 37.6−38.4 ppm) are correlated with pairs of ^{1}H resonances. These are methylene groups with nonequivalent protons. Other ^{13}C signals (δ_C = 36.8−37.6 ppm) are correlated with single ^{1}H resonances. These could be due to CH groups bound to ^{31}P, or they could be due to methylene groups having protons with nearly identical chemical shifts. In a previous publication,[10] they were originally assigned to the former. However, based on the inspection of the spectra it is not possible to determine whether the number of resonances arise from different structures **1**, **2**, and **3** in Scheme 1 or from different stereoisomers of one of these structures.

Additional information was obtained from studies on TPO-initiated poly(α-d_1-styrene) and TPO-initiated poly(β,β-d_2-styrene). The spin systems containing deuterium bound to C_α cannot be detected in the 3D SQ-HCAP experiments since this experiment selectively detects ^{1}H−^{13}C−^{31}P spin systems. Therefore, if structures **2** or **3** are present, resonances from P−CH groups will be observed in the 3D SQ-HCAP spectrum of TPO-initiated poly(β,β-d_2-styrene), but resonances from P−CH_2 groups will be absent. Likewise, in the SQ-HCAP spectrum of poly(α-d_1-styrene) resonances from P−CH_2 groups will be observed; however, signals from P−CH groups will be absent.

The 1D ^{1}H, ^{13}C, and ^{31}P spectra of TPO-initiated poly(α-d_1-styrene) are provided in the Supporting Information. The methine ^{1}H resonances near 2 ppm are greatly attenuated compared to the rest of the signals in this spectrum. A large number of small peaks are revealed in the 1.5−2.5 ppm region; these could arise from chain-end structures. Little difference is seen between the ^{13}C or ^{31}P spectra of deuterated and unlabeled polymers. The f_2f_3 (^{1}H−^{13}C) projection and individual slices from the SQ-HCAP spectrum of TPO-initiated poly(α-d_1-styrene) are essentially identical to those in the spectrum of unlabeled polystyrene (see Supporting Information). No cross-peaks were found in the 3D spectrum of poly(β,β-d_2-styrene) (not shown). This evidence proves that the chain ends contain only methylene fragments connected to ^{31}P and that structures **2** and **3** are not present in the polymer or that the amounts of structures **2** and **3** are too low to be detected in these NMR spectra. All the line broadening in the 1D spectra results from stereosequence effects in structure **1**.

Polystyrene Chain-End Conformations. In structure **1**, the methylene protons in the first monomer unit connected to ^{31}P at the chain end could have various chemical environments due to the different configurations possible on the stereogenic centers of the first few monomer units near the chain end. Even the two protons of the α-methylene groups are nonequivalent since the neighboring β-methine carbon is a stereogenic center. Scheme 2 shows the four possible triad configurations for Structure 1. They are designated as "mm", "mr", "rm", and "rr" to distinguish them from triads (mm, mr, rm, and rr) present in the polymer backbone. They are all drawn with the polymer backbone in the trans−trans (tt) conformation to help illustrate the configuration even though they might not favor this conformation.

Bovey[24] studied the 500 MHz ^{1}H NMR of poly(methyl methacrylate) (PMMA). The predominately syndiotactic polymer has mostly racemic (r) dyads which contain a 2-fold symmetry axis. Consequently, the two methylene

Scheme 2. Configurations of Chain-End Triad Structures of TPO-Initiated Polystyrene

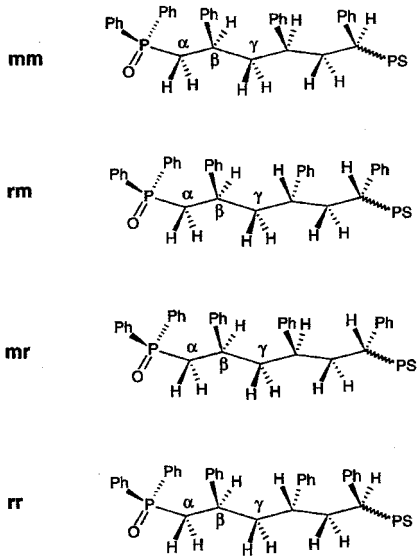

Table 1. Molecular Modeling Results for Chain-End Structures of TPO-Initiated Polystyrene

struct no.	config	conformation (probability)	H_a[a]	wgtd av	H_b[a]	wgtd av	$\langle H_a\rangle/\langle H_b\rangle$
S1	"mm"	g^+tg^+t (0.317)	0.17		0.47		
S2	"mm"	tg^-tg^- (0.317)	0.36	0.37	0.70	0.62	0.60
S3	"mm"	g^+ttg^- (0.317)	0.58		0.69		
S4	"mr"	tg^-tt (0.447)	0.63	0.37	0.46	0.43	
S5	"mr"	g^+ttt (0.447)	0.10		0.40		0.86
S6	"rm"	$tttg^+$ (0.447)	0.27	0.41	0.62	0.63	
S7	"rm"	ttg^-t (0.447)	0.55		0.63		0.65
S8	"rr"	tttt (0.698)	0.51		0.59		
S9	"rr"	g^+g^+tt (0.144)	0.37	0.50	0.50	0.60	0.83
S10	"rr"	ttg^-g^- (0.144)	0.55		0.72		

[a] Estimated uncertainty: ±0.05.

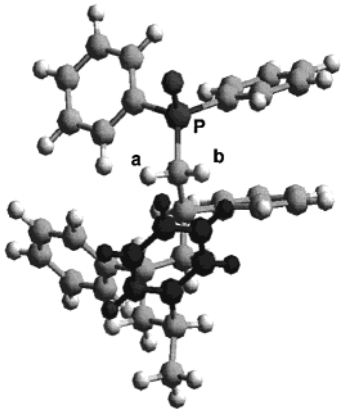

Figure 5. Simulation of S1: Chain end structure with "mm" configuration and g^+tg^+t conformation. In the figure, the phenyl ring (5) is highlighted for easier recognition.

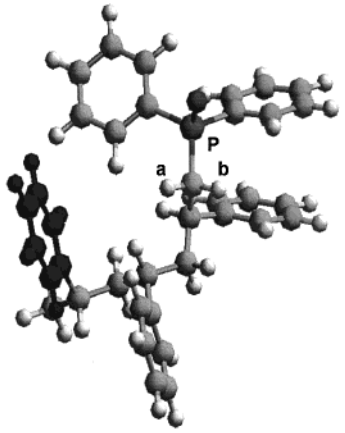

Figure 6. Simulation of S9: Chain end structure with "rr" configuration and g^+g^+tt conformation. In the figure, the phenyl ring (5) is highlighted for easier recognition.

protons are equivalent and their resonances appear as a singlet. The isotactic polymer contains meso (m) dyads which have a plane of symmetry and so the two methylene protons are nonequivalent and their resonances are observed as two doublets. In the isotactic polymer, the geminal coupling is around 15 Hz, while the two nonequivalent protons have a shift difference of 0.7 ppm.

The case of polystyrene is not as simple as that of PMMA. Here we are studying atactic polystyrene in which the number of r and m dyads are almost equal (m is about 0.45).[25] Due to the bulky phenyl side groups, the backbone conformation is not always tt. RIS calculations suggested that for meso dyads the conformational states with the highest populations are tg and gt, and for racemic dyads, the tt and gg states are predominantly populated. Although these calculations were performed for the local conformations within the polystyrene chain, they should also apply to the area near the chain end. RIS calculations on TPO-initiated polystyrene suggest 10 conformations could exist at the ^{31}P-containing chain end when considering triad configurations ("mm", "mr", "rm", and "rr"). The second and third columns in Table 1 show the 10 conformations and their probabilities as specified by the RIS of Rapold and Suter.[17] The optimized geometries of each structure were determined by using the Cerius^2 software from Molecular Simulation Inc. (MSI) based on energy minimization. Figures 5 and 6 illustrate the optimized chain end structures of S1 and S9, respectively. Only two structures are shown here to save space. It is clear from Figure 6 that the phenyl ring (5) on the third monomer unit can approach more closely to the methylene protons at the chain end than the phenyl ring (4) on the second monomer unit and will have a larger influence on the α-methylene ^{1}H chemical shifts in some conformations.

The relative shift differences of the methylene protons at each chain end of the stereosequence, labeled as H_a and H_b, were studied by evaluating the ring current shieldings as described in the Experimental Section. The ring current shielding values are summarized in the fourth and sixth columns of Table 1. Since the conformations change on a time scale much faster than the NMR time scale, only averaged values (the fifth and seventh columns of Table 1) were calculated for each triad configuration. The value $\langle H_a\rangle/\langle H_b\rangle$ indicates the degree of nonequivalence of H_a and H_b shieldings. If the ratio is near 1, the two protons will have similar chemical shifts. If the ratio is very different from 1, the two protons will have different chemical shifts. The $\langle H_a\rangle/\langle H_b\rangle$ values for the "mm" and "rm" triads are 0.60 and 0.65, and those for the "mr" and "rr" triads are 0.86 and 0.83, respectively. So the two methylene protons in "mm" and "rm" triads can be expected to have larger chemical shift differences than those in "mr" and "rr" triads

Figure 7 shows selected f_2f_3 (^{1}H−^{13}C correlations) slices from the 3D SQ-HCAP spectrum at the eight

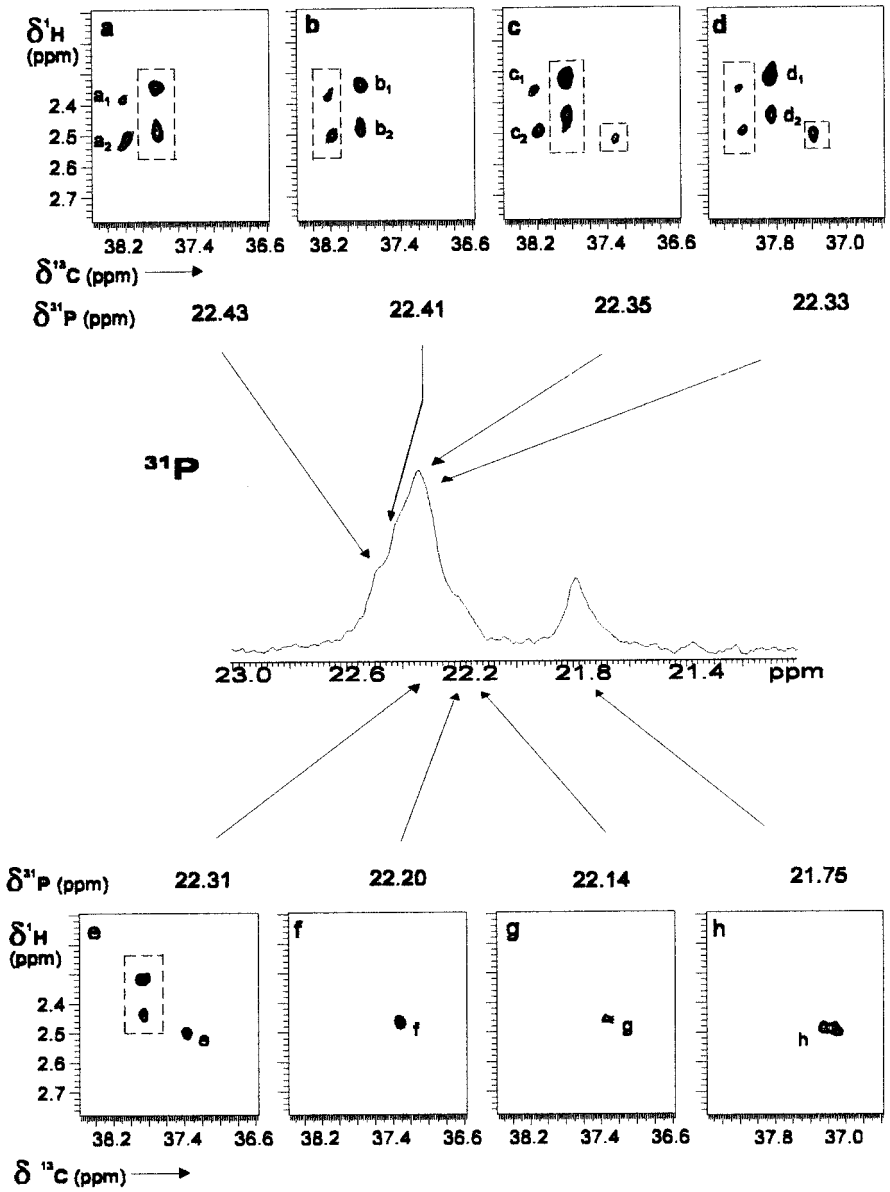

Figure 7. Selected f_2f_3 ($^1H-^{13}C$) slices from the 3D SQ-HCAP spectrum of TPO-initiated polystyrene. The resonances within the dashed lines are from signals bleeding through from adjacent slices.

resolved ^{31}P chemical shifts of unlabeled polystyrene. The cross-peaks in each of these slices are well resolved and all result from chain end CH_2 fragments directly bonded to the ^{31}P whose shift corresponds to the position of the slice in the 3D spectrum. The strong backbone C−H correlations are filtered from the spectrum. Because the 3D SQ-HCAP NMR spectra of unlabeled polystyrene and poly(α-d_1-styrene) are identical, these signals are believed to arise from the eight major stereoisomers of structure **1**, which can be distinguished by 3D NMR.

In the spectra, two types of methylene C−H correlations are detected. One group has pairs of cross-peaks at each ^{13}C chemical shift. These are shown across the top of Figure 7. The second group has a single cross-peak at each ^{13}C chemical shift. These are aligned across the bottom of Figure 7. On the basis of the RIS calculations described above, the cross-peaks in the top four slices are attributed to "mm" and "rm" triads because these geminal methylene protons have large ^1H chemical shift differences (around 0.15 ppm). The cross-peaks in the lower four slices are attributed to "mr" and "rr" chain-ends because the methylene carbons are each correlated to single ^1H chemical shifts. The chemical shifts and triad resonance assignments are summarized in Table 2. Since the resonances of eight $^{31}P-CH_2$ sets of correlations are resolved by 3D NMR, the shifts of the chain end atoms are dependent on the stereochemistry of at least the first four monomer units on the polymer chain. At this time, it is hard to say which slice is attributed to which structure based solely on RIS calculations and predictions of ^1H chemical shift differences. The NMR 3D-CT-HCCH NMR studies of poly(α,*β*-$^{13}C_2$-styrene) initiated by TPO can help to answer this question.

Poly(α,*β*-$^{13}C_2$-styrene) Initiated by TPO. While 3D CT-HCCH NMR might be performed on unlabeled polystyrene, the experiment involves selective detection of resonances from $^1H-^{13}C-^{13}C-^1H$ spin systems. At natural abundance, these systems constitute only 0.01% of the molecules. NMR signals are further attenuated by the presence of many chain-end

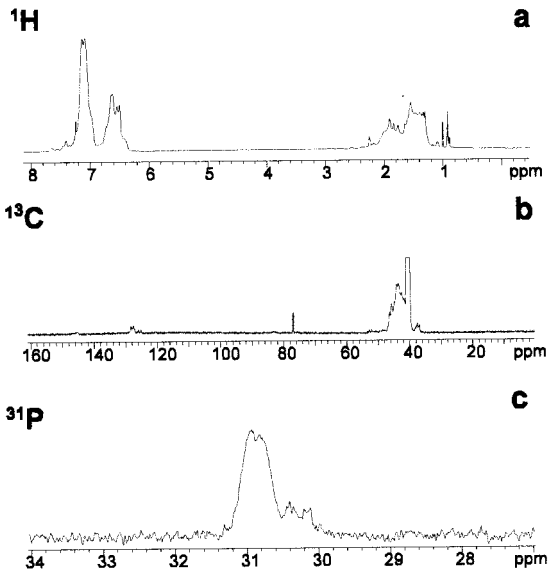

Figure 8. 1D NMR spectra of TPO-initiated poly(α,*β*-$^{13}C_2$-styrene): (a) 750 MHz ^{1}H, b) 188 MHz ^{13}C, and (c) 121 MHz ^{31}P.

Table 2. Chemical Shifts and Triad Resonance Assignments for Polystyrene and Poly(α-*d*$_1$-styrene)

		polystyrene			poly(α-d$_1$-styrene)		
cross peaks	triad assignments	$\delta(^1H)$ (ppm)	$\delta(^{13}C)$ (ppm)	$\delta(^{31}P)$ (ppm)	$\delta(^1H)$ (ppm)	$\delta(^{13}C)$ (ppm)	$\delta(^{31}P)$ (ppm)
a_1	"mm" or "rm"	2.38	38.23	22.43	2.33	38.00	22.45
a_2		2.53	38.23	22.43	2.48	38.00	22.45
b_1		2.34	37.86	22.41	2.31	37.72	22.43
b_2		2.48	37.86	22.41	2.45	37.72	22.43
c_1		2.36	38.20	22.35	2.34	38.00	22.39
c_2		2.50	38.20	22.35	2.48	38.00	22.39
d_1		2.31	37.86	22.33	2.30	37.74	22.37
d_2		2.44	37.86	22.33	2.43	37.74	22.37
e	"mr" or "rr"	2.50	37.38	22.31	2.48	37.25	22.33
f		2.47	37.32	22.20	2.47	37.03	22.27
g		2.49	36.82	21.80	2.43	37.15	22.17
h		2.49	37.18	21.75	2.51	36.95	21.75

structures. There are eight phosphorus-containing structures as well as numerous stereoisomers for each of the structures in Scheme 1. By preparing polystyrene from 95% α,*β*-$^{13}C_2$-styrene, the signals of interest from the polymer backbone atoms are enhanced 10 000-fold.

The 1D ^{1}H, ^{13}C, and ^{31}P spectra of TPO-initiated poly(α,*β*-$^{13}C_2$-styrene) are shown in Figure 8. The aliphatic peaks in the ^{1}H spectrum exhibit splittings from J_{HC} due to the ^{13}C enrichment. The ^{31}P spectrum exhibits broad and weak signals because of numerous one-bond and multiple bond J_{CP} couplings. The signals in the aliphatic region of the ^{13}C spectrum are dramatically enhanced relative to those in the aromatic region. The f_2f_3 projection (^{1}H−^{13}C) correlations (see Supporting Information) from the CT-SQ-HCAP spectrum of TPO-initiated poly(α,*β*-$^{13}C_2$-styrene) is essentially identical to the SQ-HCAP spectrum of unlabeled polystyrene in Figure 4. Constant time chemical shift evolution (t_2) in the ^{13}C dimension is necessary for observing clean spectra from samples with ^{13}C enrichment since it eliminates homonuclear ^{13}C−^{13}C couplings during the ^{13}C chemical shift evolution delay.

The f_2f_3 (^{1}H−^{13}C) slices from the 3D CT-SQ-HCAP spectrum of poly(α,*β*-$^{13}C_2$-styrene) at each of the eight ^{31}P chemical shifts (Figure 9) are essentially identical to those in the 3D SQ-HCAP spectrum of unlabeled polystyrene shown in Figure 7. However, they have far better signal-to-noise as a consequence of the labeling. The spectral interpretations described above for unlabeled polystyrene applies to the interpretation of the spectrum of poly(α,*β*-$^{13}C_2$-styrene) as well.

Once the assignment of the C_α resonances are determined (in the remaining discussion a Greek letter subscript will be used to refer to the position of a backbone carbon relative to the chain-end ^{31}P atom), the CT-HCCH experiment can be used to establish the $C_\alpha-C_\beta-C_\gamma$ sequence of one-bond connectivities and to obtain resonance assignments for C_β and C_γ. Once these assignments are obtained, the sequence of CH−CH_2 attachments can be determined in order to prove the head-to-tail connectivity of the first two monomer units in the chain. The ability to use 3D NMR to resolve geminal methylene resonances of the protons bound to these carbons also provides a means of measuring their chemical shift differences. This in turn provides a way to determine the stereochemistry of the next dyad in the polymer chain. Figures 10 and 11 illustrate the combined use of the CT-SQ-HCAP data and CT-HCCH data to identify the resonances of the first monomer units along the polymer backbone. The figures contain selected slices from these two 3D experiments. The CT-HCCH spectrum is not very clean because it contains many other signals from the rest of the polymer chain. Fortunately the C_β and C_γ signals are resolved from the strong signals from the rest of the main chain. On the basis of RIS calculations and the subsequent chemical shielding calculations, it may be concluded when the configuration of the first dyad is m, then the two protons attached to the γ carbon should be nonequivalent and can be expected to have a large chemical shift difference. On the other hand, if the configuration in the first dyad is r, then the γ methylene protons should be nearly equivalent and are expected to give a smaller shift differences. The 3D CT-HCCH spectrum is helpful to track the shifts of protons connected to the γ carbon through the α, β, and γ carbon connectivities.

Although the f_1f_2 slices from the CT-HCCH spectrum are like 2D INADEQUATE spectra in that they provide information about ^{13}C connectivity, examination of the f_2f_3 slices can be more beneficial. These slices show correlations between the ^{1}H and ^{13}C DQ chemical shifts. The ^{13}C SQ resonances exhibit more chemical shift dispersion than ^{1}H resonances. This makes slice selection easier, with less bleed-through of signals from adjacent slices. In the f_2f_3 slices, two sets of resonances are expected in one slice from the spectrum of a linear hydrocarbon chain. Because the phenyl side groups are not ^{13}C labeled, signals from correlations to atoms in the side groups need not be considered, (since they are attenuated 100 fold relative to the signals from the backbone atoms). These sets of resonances correlate two ^{1}H resonances, which are attached to two adjacent ^{13}C atoms, at the ^{13}C DQ resonance frequency corresponding to the sum of the two ^{13}C resonances. Therefore, in a linear hydrocarbon up to three adjacent ^{1}H resonances can be observed in each slice. In addition, since the ^{13}C DQ frequency evolves twice as fast as the ^{13}C SQ frequency, these slices have a better potential to eliminate problems from overlapping resonances.

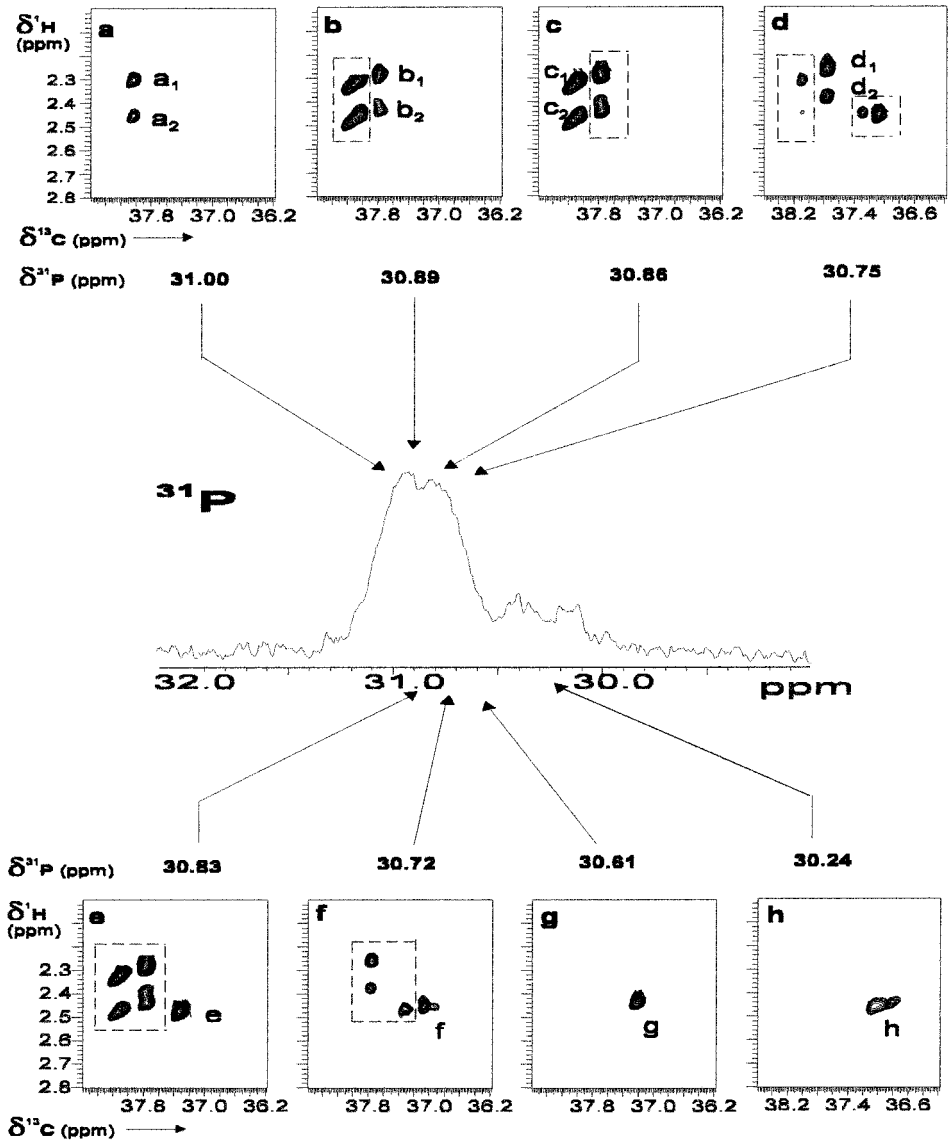

Figure 9. Selected f_2f_3 ($^1H-^{13}C$) slices from the 3D CT-SQ-HCAP spectrum of TPO-initiated poly(α,β-$^{13}C_2$-styrene). The resonances within the dashed lines are from signals bleeding through from adjacent slices.

The resonance assignments begin with the identification of a ^1H and ^{13}C correlation from a methylene group directly bound to ^{31}P atom in the CT-SQ-HCAP spectrum. The f_1f_3 slice from the CT-HCAP spectrum (Figure 10a, $\delta_{C\alpha} = 38.0$ ppm) is used to identify the resonances $\alpha_{1(ac)}$ and $\alpha_{2(ac)}$ as two $^{31}P-^{13}CH_2$ fragments, which produce cross-peaks a_1/a_2 and c_1/c_2 (shown in Figure 7, parts a and c). The next CH fragments can be indentified by locating the methylene ^1H resonances bonded to C_α in the f_2f_3 slices from CT-HCCH spectrum at the ^{13}C SQ chemical shift of C_α (Figure 10b). From this slice, the connectivity between C_α and C_β is proven, and C_β and H_β are identified by the C−H correlation sharing the same ^{13}C DQ frequency as the C_α and H_α atoms. Since C_α is not coupled to other ^{13}C nuclei, cross-peak β_{ac} is the only correlation found in this slice. The slices in Figures 10c and 10d come from the same plane of the CT-HCCH spectrum at ^{13}C SQ chemical shift of $C_\beta = 37.9$ ppm. Figure 10c shows exactly the same correlations between C_α and C_β as those in Figure 10b. Additionally, there are three more cross-peaks found in Figure 10d. The lowest signal originates from C_β which occurs at the proton shift of H_β. The other two correlations must originate from the γ-CH_2 fragment because they produce cross-peaks at the same ^{13}C DQ coherence frequency as C_β. Since the two protons on C_γ are nonequivalent, they appear as a pair of cross-peaks, labeled as $\gamma_{1(ac)}$ and $\gamma_{2(ac)}$ in Figure 10d. In this way, C_γ and H_γ are identified. The shift difference between cross-peaks $\gamma_{1(ac)}$ and $\gamma_{2(ac)}$ is 0.59 ppm.

The same tracking method applies to the other α-CH_2 resonances in Figure 7. Parts e−h of Figure 10 show the $C_\beta-H_\beta$, $C_\gamma-H_\gamma$ correlation for the mainchain CH_n groups attached to the α-CH_2 which produces the cross-peaks labeled as b_1/b_2 and d_1/d_2 in Figure 7, parts b and d. Cross-peaks $\gamma_{1(bd)}$ and $\gamma_{2(bd)}$ have $\Delta\delta_H = 0.43$ ppm. This value is smaller than that for the γ-protons producing the cross-peaks in Figure 10d. Therefore, it is reasonable to assign the cross-peaks a_1/a_2 and c_1/c_2 to "mm" triads and cross-peaks b_1/b_2 and d_1/d_2 to "rm" triads.

The identification of the resonances of C_γ and H_γ from the chain end structures whose C_α and H_α cross-peaks are labeled as e and g in Figure 7 is shown in Figure 11, parts a−d, and for f and h is shown in Figure 11, parts e−h. The ^1H shift differences are 0.36 and 0.62

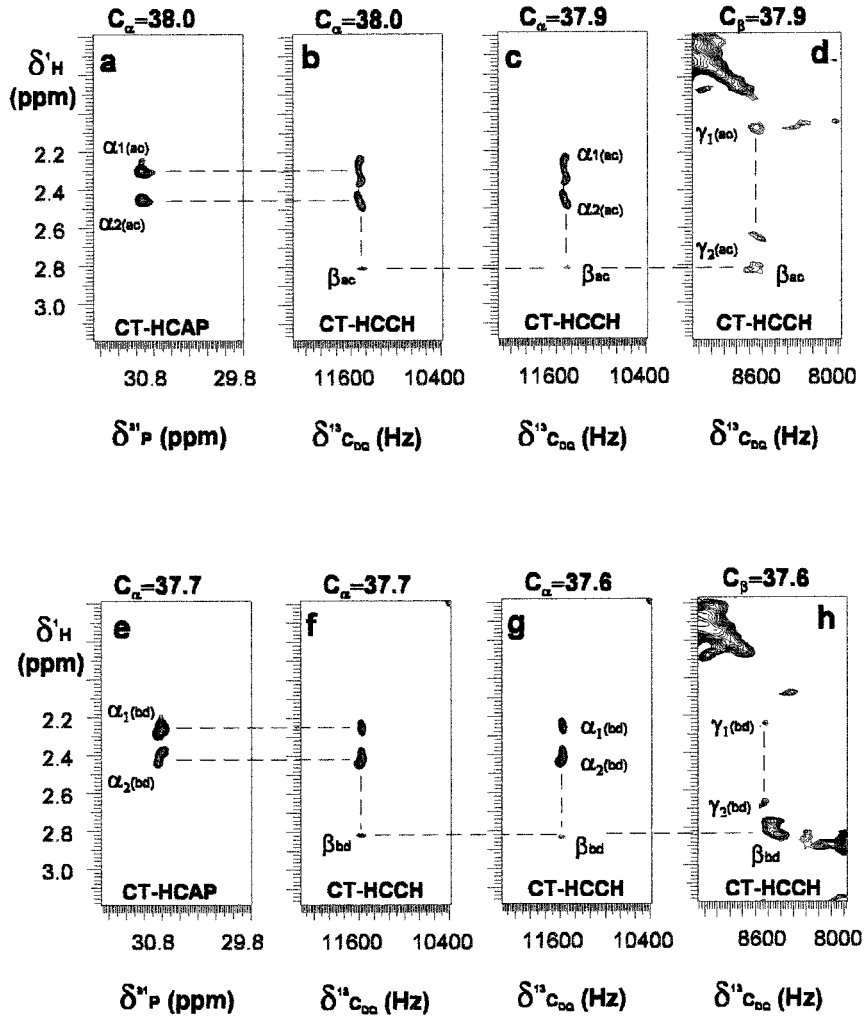

Figure 10. Slices from the CT-SQ-HCAP and CT-HCCH spectra of TPO-initiated poly(α,β-$^{13}C_2$-styrene). The dashed lines indicate the carbon connectivities from C_α through C_γ. The resonances $\alpha_{1(ac)}$ and $\alpha_{2(ac)}$ ($\delta_{C\alpha}$ = 38.0 ppm) in the top four slices come from two $^{31}P-^{13}CH_2$ fragments which produce cross-peaks a_1/a_2 and c_1/c_2 shown in Figure 7, parts a and c. The resonances $\alpha_{1(bd)}$ and $\alpha_{2(bd)}$ ($\delta_{C\alpha}$ = 37.7 ppm) in the bottom four slices come from two $^{31}P-^{13}CH_2$ fragments which produce cross-peaks b_1/b_2 and d_1/d_2 shown in Figure 7, parts b and d.

ppm, respectively. Therefore, resonances e and g are assigned to "rr" triads and resonances f and h are assigned to "mr" triads.

There are now two groups of resonances assigned to each triad structure. To further differentiate between the structures in each of these groups, tetrad structures which are determined by the configuration of the third monomer unit must be considered. RIS calculations become unreliable because of the small differences caused by the configuration of the chiral center of the monomer unit three units away. For example, the ^1H and ^{13}C chemical shifts of cross-peaks a_1/a_2 "mm" and c_1/c_2 "mm" are almost identical. While these signals arise from "mmm" and "mmr" tetrads, it is not possible to unambiguously identify the two sets of resonances. Similarly, cross-peaks b_1/b_2 or d_1/d_2 come from "rmm" and "rmr" tetrads. Tentative tetrad assignments for all the cross-peaks e, g, f, and h shown in Figures 10 and 11 are summarized in Table 3.

Conclusion

The chain-end structures of polystyrene were characterized by using a combination of 750 MHz 3D NMR experiments. High field 3D NMR techniques provide much better resolved spectra, enabling us to assign the chain-end structures up to the triad level with the help of RIS calculations. The dispersion in the 3D spectra permit resolution of resonances from the chain-end structures up to the tetrad level. Data from two 3D experiments were combined to make assignments of the resonances originating from minor structures (chain-end) in polystyrene, which are present in very low concentration compared with the backbone repeat units.

Isotopic labeling with ^{13}C is utilized together with 3D-NMR in this work to obtain information on resonance assignments of C_β and C_γ along the chain end in addition to the C_α directly bound to the ^{31}P atom. Deuterium-labeling techniques were also used to prepare polystyrenes. In addition to unlabeled polystyrene, poly(α-d_1-styrene) and poly(β,β-d_2-styrene) were investigated under the same NMR conditions. By comparison of the 3D SQ-HCAP spectra of these three samples, one can distinguish between signals originating from CH_2 and CH groups bound to ^{31}P. It turned out that all the resonances are from CH_2 groups, proving that one mechanism is dominant for polymer initiation, i.e., the addition of TPO radical to the β-carbon of styrene monomers. Since signals from $^{31}P-CH$ structure fragments were not detected,[26] the diphenylphosphinyl

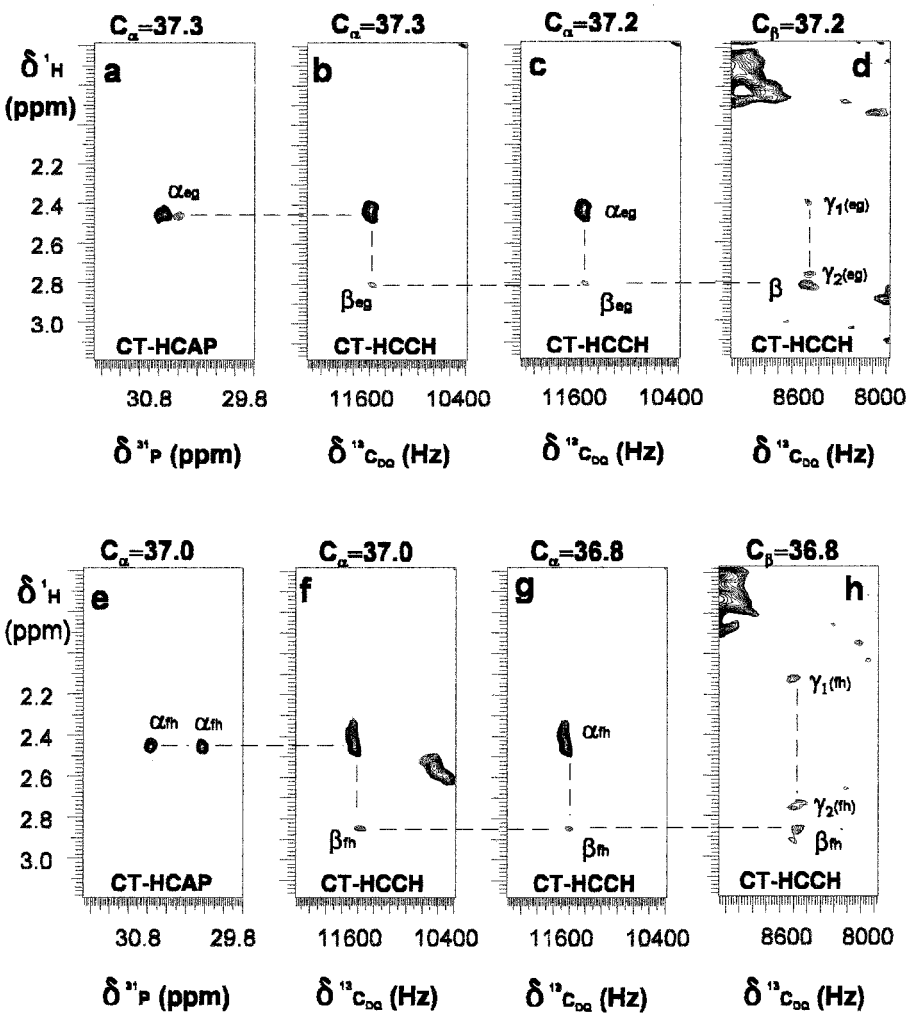

Figure 11. Slices from the CT-SQ-HCAP and CT-HCCH spectra of TPO-initiated poly(α,β-$^{13}C_2$-styrene). The dashed lines indicate the carbon connectivities from C_α through C_γ. The resonances α_{eg} ($\delta_{C\alpha}$ = 37.3 ppm) in the top four slices come from two $^{31}P-^{13}CH_2$ fragments which produce cross-peaks e and g shown in Figure 7, parts e and g. The resonances α_{fh}($\delta_{C\alpha}$ = 37.0 ppm) in the bottom four slices come from two $^{31}P-^{13}CH_2$ fragments which produce cross-peaks f and h shown in Figure 7, parts f and h.

Table 3. Chemical Shifts and Tetrad Resonance Assignments of Polystyrene Chain Ends on TPO-Initiated Poly(α,β-$^{13}C_2$-Styrene).

		poly(α,$\beta^{-13}C_2$styrene)		
cross peaks	tetrad assignments	$\delta(^1H)$ (ppm)	$\delta(^{13}C)$ (ppm)	$\delta(^{31}P)$ (ppm)
a_1	mmm/mmr	2.30	38.11	31.00
a_2		2.46	38.11	31.00
b_1	rmm/rmr	2.29	37.74	30.89
b_2		2.44	37.74	30.89
c_1	mmm/mmr	2.33	38.11	30.86
c_2		2.47	38.11	30.86
d_1	rmm/rmr	2.27	37.74	30.75
d_2		2.38	37.74	30.75
e	rrm/rrr	2.47	37.30	30.83
f	mrm/mrr	2.46	37.04	30.72
g	rrm/rrr	2.43	37.30	30.61
h	mrm/mrr	2.46	37.00	30.24

radical does not add to a significant extent to the α-carbon of styrene during the initiation of polymerization, nor does it play a significant role in the termination step as originally thought.10 Similar 3D-NMR studies using ^{13}C-labeled benzoyl groups on TPO may reveal its role in the initiation and termination steps of styrene polymerization.

Acknowledgment. We wish to acknowledge the National Science Foundation (DMR-9310642, DMR-9523278, and DMR-9617477) for support of this research, and the Kresge Foundation and donors to the Kresge Challenge program at the University of Akron for funds used to purchase the 750 MHz instrument used in this work.

Supporting Information Available: Figures showing 1D and 3D NMR data of poly(α-d_1-styrene) and poly(α,β-$^{13}C_2$-styrene). This material is available free of charge via the Internet at http://pubs.acs.org.

References and Notes

(1) Moad, G.; Solomon, D. H.; Willing, R. *Macromolecules* **1984**, *17*, 1094.
(2) Bevington, J. C.; Ebdon, J. R.; Huckerby, T. N. *Polym. Commun.* **1985**, *23*, 163.
(3) Bevington, J. C.; Ebdon, J. R.; Huckerby, T. N. *Eur. Polym. J.* **1984**, *20*, 645.
(4) Kristina, J.; Moad, G.; Solomon, D. H. *Eur. Polym. J.* **1989**, *25*, 767.
(5) Medsker R. E.; Chumacero, M.; Santee, E. R.; Sebenik, A.; Harwood: H. J. *Acta Chim. Slov.* **1998**, *45* (4), 371.
(6) Rollins, P. Ph.D. Dissertation, The University of Akron, August, 1998.
(7) Jacobi, M. Henne, A. J. *Radiat. Curing* **1983**, *10*, 16.
(8) Schnabel, L.; Sumiyoshi, T. *Polymer* **1985**, *26*, 141.

(9) Busfield, K. W.; Grice, D. I.; Jenkins, I. D. *Aust. J. Chem.* **1995**, *48* (3), 625.
(10) Rinaldi, P. L.,; Saito, T.; Harwood: H. J. *J. Magn. Reson. Ser. A* **1996**, *120*, 125.
(11) Dietliker, K.; Kolczak, U.; Rist, G.; Wirz, J. *J. Am. Chem. Soc.* **1996**, *118*, 6477.
(12) Deuterated and ^{13}C-enriched styrenes and polymers derived from them will be named the conventional way with α and *β* representing the methine and methylene carbons or deuterium atoms. When the spectra of the polymers are discussed, descriptions C_α, C_β, and C_γ will be used to represent the carbons that are separated from phosphorus by one, two, or three bonds, respectively.
(13) Ikura, M.; Kay, L. E.; Bax, A. *Biochemistry* **1990**, *29*, 4659.
(14) Shaka, A. J. Barker, P. B. Freeman, R. *J. Magn. Reson.* **1985**, *64*, 547.
(15) Saito, T.; Rinaldi, P. L. *J. Magn. Reson.* **1998**, *132*, 41.
(16) Fujiwara, T. Anai, T. Nagayama, K. *J. Magn. Reson., Ser. A* **1993**, *104*, 103.
(17) Rapold, R. F.; Suter, U. W. *Macromol. Theory Simul.* **1994**, *3*, 1.
(18) Rehan, M.; Mattice, W. L.; Suter, U. W. *Adv. Polym. Sci.* **1997**, *131/132*, A050.
(19) Mattice, W. L.; Suter, U. W. *Conformational Theory of Large Molecules. The Rotational Isomeric State Model in Macromolecular Systems*; Wiley: New York, 1994; pp 174−175.
(20) Bovey, F. A. *Nuclear Magnetic Resonance Spectroscopy*; Academic Press: New York, 1969; pp 64−65 and 264−274.
(21) Morris, G. A.; Freeman, R. *J. Am. Chem. Soc.* **1979**, *101*, 760.
(22) Mhller, L. *J. Am. Chem. Soc.* **1979**, *101*, 4481.
(23) Bax, A.; Freeman, R.; Kempsell, S. P. *J. Am. Chem. Soc.* **1980**, *102*, 4849.
(24) Bovey, F. A.; Schilling, F. C.; Mirau, P. A. *Polym. Prepr. (Am. Chem. Soc., Div. Polym. Chem.)* **1989**, *30* (2), 431.
(25) Harwood: H. J.; Chen, T. K. *ACS Symp. Ser.* **1984**, *247*, 197.
(26) The NMR samples consisted of approximately 100 mg of polymer (maximum number average molecular weight of approximately 9000) dissolved in 0.7 mL of solvent. Although the NMR results were not rigorously quantitative, the detection limit can be estimated by considering the fact that there are several phosphorus-containing chain-end species present, the lowest concentration species is approximately 5−10% of the mixture, and P−CH chain ends could have easily been detected at concentrations two to three times lower.

MA000898C